LANGMUIR Article
Cite This: Langmuir 2018, 34, 3289−3295
pubs.acs.org/Langmuir

Photochemically Powered AgCl Janus Micromotors as a Model System to Understand Ionic Self-Diffusiophoresis

Chao Zhou,[†] H. P. Zhang,[‡,§] Jinyao Tang,[∥] and Wei Wang*[,†]

[†]School of Materials Science and Engineering, Harbin Institute of Technology (Shenzhen), Shenzhen 518055, China
[‡]School of Physics and Astronomy and Institute of Natural Sciences, Shanghai Jiao Tong University, Shanghai 200240, China
[§]Collaborative Innovation Center of Advanced Microstructures, Nanjing 210093, China
[∥]Department of Chemistry, University of Hong Kong, Hong Kong SAR 999077, China

Supporting Information

ABSTRACT: Micromotors are an emerging class of micromachines that could find potential applications in biomedicine, environmental remediation, and microscale self-assembly. Understanding their propulsion mechanisms holds the key to their future development. This is especially true for a popular category of micromotors that are driven by asymmetric surface photochemical reactions. Many of these micromotors release ionic species and are propelled via a mechanism termed "ionic self-diffusiophoresis". However, exactly how it operates remains vague. To address this fundamental yet important issue, we have developed a dielectric-AgCl Janus micromotor that clearly moves away from the AgCl side when exposed to UV or strong visible light. Taking advantage of numerical simulations and acoustic levitation techniques, we have provided tentative explanations for its speed decay over time as well as its directionality. In addition, photoactive AgCl micromotors demonstrate interesting gravitactic behaviors that hint at three-dimensional transport or sensing applications. The current work presents a well-controlled and easily fabricated model system to understand chemically powered micromotors, highlighting the usefulness of acoustic levitation for studying active matter free from the effect of boundaries.

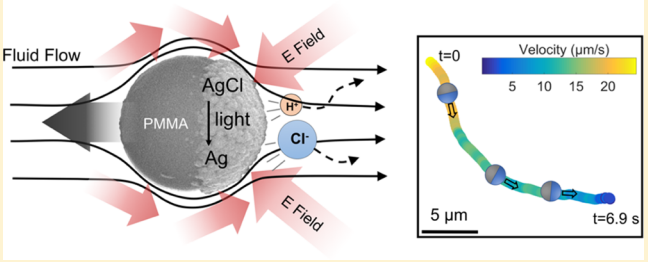

INTRODUCTION

Understanding and exploiting powered motion at small scales sits at the core of a number of fundamental and applied research areas, such as active matter,[1] micromachines,[2,3] microbiology,[4,5] and nanomedicine.[6−9] Although the dynamics of microorganisms (such as cells and bacteria) and protein motors (such as kinesins and myosins) are largely understood, progress in mimicking such a biological motion with synthetic microswimmers has been small, until the introduction of catalytic bimetallic micromotors about 15 years ago.[10,11] Since then, a myriad of micromotors have been developed with various mechanisms and versatile functionalities (see, e.g., refs[7,12−16] and references therein).

Among them, chemical reactions remain a popular choice for powering micromotors,[17−19] and many rely heavily on local chemical gradients.[13] Colloids are long known to move in externally applied chemical gradients, a mechanism termed "diffusiophoresis",[20,21] but autonomously moving micromotors are unique for they generate their own chemical gradients locally. This is conveniently termed "self-diffusiophoresis"[22] and is often induced by an asymmetric surface reaction that consumes and releases chemical species. This reaction can be spontaneous, such as the dissolution of a weakly soluble salt in water[23,24] or the enzymatic conversion of a substrate molecule,[25−28] or it can be initiated via external stimuli, light being a prominent example.[29,30]

Given that light can be remotely applied and easily tuned in both wavelength and intensity, light-powered micromotors are quickly gaining popularity.[14,31] Many of these micromotors involve a photochemical reaction that generates a local chemical gradient and therefore moves by self-diffusiophoresis. A quick survey of literature presents a few notable examples based on Janus structures, with parts of the particles being photochemically active. These include SiO_2−Ag,[32] TiO_2−SiO_2,[29] silver-Dynabead Janus spheres,[33] and AgCl-AFP dimers,[34] all of which move unidirectionally when exposed to ultraviolet (UV) light. The other important and common feature of these systems is that they all produce ionic species, which give rise to ionic self-diffusiophoresis that is responsible for the operation of a large portion of existing micromotors. Yet, its operation mechanism still remains to be clarified. Unfortunately, the existing literature can provide only limited insight into this issue because of practical complications including complex particle shapes, poor visual contrast to distinguish motor directionality, slow propulsion speed, and the

Received: December 20, 2017
Revised: February 10, 2018
Published: February 13, 2018

DOI: 10.1021/acs.langmuir.7b04301
Langmuir 2018, 34, 3289−3295

existence of multiple possible driving mechanisms, to name a few (see Supporting Information for a detailed discussion). The elucidation of ionic self-diffusiophoresis is often further hindered by the presence of boundaries and possible electro-osmotic flows as a result.

As an effort to build a simple yet reliable model system to understand ionic self-diffusiophoresis, we here report an AgCl Janus micromotor powered by photochemical reactions, drawing inspirations from an earlier study by Ibele and co-authors.[34] When irradiated with light, this Janus particle moves away from the reacting (AgCl) side and shows negative gravitaxis. Finite element simulation suggests that the near-field electric field pointing from the inert to the reacting side could be the main phoretic force that propels this Janus particle to move away from the AgCl side. Our finding introduces a photochemical micromotor with well-controlled kinetics and interesting gravitactic behaviors and presents a renewed and microscopic view of ionic self-diffusiophoresis that applies to a wide variety of micromotors.

EXPERIMENTAL SECTION

Sample Synthesis and Fabrication. The monolayer of poly(methyl methacrylate) (PMMA) microspheres was obtained following ref 35. A concentrated suspension of PMMA particles in ethanol was added to the surface of a thin layer of hexane floating on water. The particles spontaneously formed a monolayer. The liquid was later pipetted out, and the monolayer was transferred to a flat substrate (e.g., silicon wafer). A thin layer (50 nm) of silver was then thermally evaporated by electron beam in a vacuum onto this monolayer of beads (e-beam evaporator HHV TF500). Silver was converted into silver chloride by immersing the silicon wafer carrying the microsphere monolayer into $FeCl_3$ solutions (0.01 mol/L, at room temperature for 20 min). A small amount of polyvinylpyrrolidone (PVP, 0.025 mol/L monomer concentration) was also added into the solution to produce fine crystals of AgCl. The AgCl morphology with and without the addition of PVP is shown in Figure S1 in the Supporting Information. Although the crystals differed in morphology, their behaviors under UV light were qualitatively the same. Crystalline information and chemical composition of the synthesized PMMA−AgCl Janus particles can be found in Figure S2.

Motor Experiment. In a typical experiment, the Janus particles were suspended in deionized water. The suspension was transferred into a rectangular capillary tube (VitroCom, model 3520, thickness 200 μm) and observed under either an upright optical microscope (Olympus BX51M) or an inverted optical microscope (Olympus IX73). Because of gravity, the particles mostly sediment to the bottom of the experiment cell (the capillary tube), and videos were usually recorded at this plane. However, when irradiated with light, the particles could float upward and eventually became trapped at the "ceiling" of the capillary tube (negative gravitaxis, discussed below). The optical microscope was equipped with a dual-housing adapter (model U-DULHA, Olympus) so that both the halogen lamp and the mercury lamp could be turned on or be switched from one to the other when needed. Videos were taken by a Point Grey camera mounted on the microscope (model FL3-U3-13E4C-C) at a frame rate of 30 frames per second, and either a 20× or a 50× objective lens was used. The videos were then processed and analyzed by MATLAB. Particle coordinates were obtained, and their trajectories and speeds can therefore be calculated.

Ultrasound Experiments. The ultrasonic manipulation device was fabricated based on previous reports.[12,36] The setup was constructed by attaching a piece of lead zirconate titanate ceramic disk (STEMINC, part no. SMD12T06R412WL, resonance frequency 3.4 MHz) to the back of a silicon wafer with epoxy resin. On its front side, the experimental chamber (usually a rectangular capillary tube from Vitrocom) was fixed by ultrasound gels directly above the ceramic disk. During the experiment, a function generator (Agilent 33210A) sent a sinusoidal signal to the piezoelectric disk, which produced ultrasound that propagated through the aqueous microparticle suspension in the acoustic cell. At the resonance frequency, typically 3−4 MHz for our setup, the particles floated up to the levitation plane at the center of the acoustic cell and moved on this plane. The acoustic forces exerted on the particle is very sensitive to the driving frequency and voltage, and one can tune it carefully so that the particles are levitated, yet their light-powered autonomous motion is minimally affected by acoustic forces. Therefore, unlike metallic microrods that show fast autonomous motion along their long axis in the same ultrasound setup,[36] PMMA−AgCl Janus particles are not actively propelled by ultrasound used in our experiment.

Numerical Simulations. To understand how the surface photochemical reaction provides prolusion to a PMMA−AgCl particle, we have used a model originally developed by Velegol et al. for the study of self-electrophoretic micropumps[37] but more recently adapted by Velegol et al. and Zhang et al. for the study of self-electrophoretic swimmers near a wall.[38,39] Unlike the Janus particle in the previous models that releases and consumes ionic fluxes at each of the hemisphere, respectively, the Janus particle in our model produces H^+ and Cl^- ions at a flux of J only at its AgCl hemisphere, whereas the PMMA sphere is chemically inert. The electrical double layer (EDL) of the particle is assumed to be infinitely thin and not significantly perturbed by the surface reactions. The electrical boundary condition at the double layer of the AgCl hemisphere is set by the normal potential gradients $-(\partial\phi/\partial n) = Jk_BT/2en_0\,(1/D^+ - 1/D^-)$, where ϕ is the electrical potential, k_B is the Boltzmann constant, T is the temperature, e is the proton charge, n_0 is the bulk concentration of ions, and D^+ and D^- are the diffusion coefficients of H^+ and Cl^-, respectively. The electrical boundary condition at the double layer of PMMA hemisphere is $-(\partial\phi/\partial n) = 0$. Outside EDL, it is electrically neutral, and the electrostatic problem is solved by the Laplace equation ($\nabla^2\phi = 0$). Fluid flows outside EDL are governed by the Stokes flow: $\eta\nabla^2\boldsymbol{u} = 0$ and $\nabla\cdot\boldsymbol{u} = 0$, where η is the dynamic viscosity of the solution and $\boldsymbol{u}$ is the fluid speed. On the surface of the PMMA−AgCl, however, the flow boundary condition is governed by an electro-osmotic slip velocity $U_{eo} = \zeta\varepsilon E'/\eta$, where ε is the medium permittivity and E' is the tangential component of the local electric field. The two hemispheres carry zeta potentials of ζ_{AgCl} and ζ_{PMMA}, respectively. Finally, the speed of the Janus particle can be calculated in one of three ways, the details of which can be found in the Supporting Information.

This model was solved by a finite element package (COMSOL Multiphysics 5.2a) in a two-dimensional (2D) axisymmetric configuration. In the simulation model, a sphere of 2.5 μm in diameter is placed at the center of a cylinder of 100 μm in length and 100 μm in diameter. An estimated ionic flux J of 1.6×10^{-5} mol/(m^2 s) was used. Details of model implementation, parameter selection and estimations, and meshing conditions are given in the Supporting Information.

RESULTS AND DISCUSSION

The fabrication of the Janus microparticles is illustrated in Figure 1a. Briefly, PMMA microspheres of 2.5 μm in diameter were coated by a 50 nm layer of silver, which was then converted to silver chloride (AgCl) by iron(III) chloride ($FeCl_3$) solution.[40] The as-synthesized Janus particle had a zeta potential of −35.1 ± 3.1 mV. Details of fabrication and characterization can be found in the Experimental Section and the Supporting Information.

When irradiated with UV light (~1.4 W/cm^2), these PMMA−AgCl particles moved in water at considerable speeds away from the AgCl side; at long time intervals, their trajectories became Brownian (Figure 1b and Video S1). Interestingly, unlike many reported micromotors that more or less maintain a constant speed over time, PMMA−AgCl micromotors slowed down within ~10 s in a gradual and regular way until Brownian motion took over (Figure 1c,d, Video S2). Although speed decrease is often considered a

DOI: 10.1021/acs.langmuir.7b04301
Langmuir 2018, 34, 3289−3295

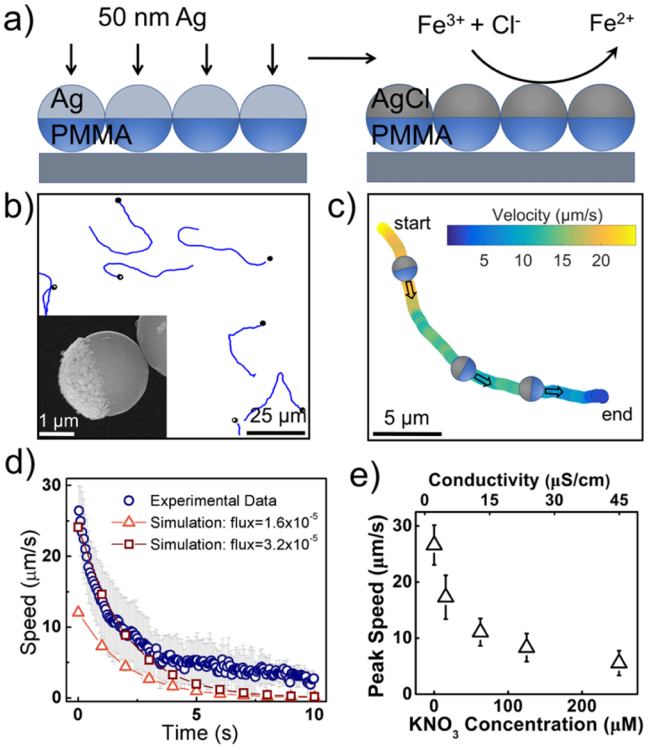

Figure 1. Dynamics of PMMA–AgCl micromotors under light. (a) Fabrication scheme of PMMA–AgCl Janus particles. (b) Particle trajectories in 7.3 s under light. Inset: A scanning electron micrograph of a PMMA–AgCl Janus particle. (c) Representative trajectory of a PMMA–AgCl micromotor of decreasing speeds (color-coded) over 6.9 s. (d) Experimental speed decay profile of a Janus micromotor in 10 s (circles), with speeds simulated at surface fluxes of 1.6×10^{-5} (triangles) and 3.2×10^{-5} mol/(m^2 s) (squares). (e) Motor peak speeds as a function of solution conductivity.

disadvantage for micromotor applications, why and how the micromotor slows down can provide us with valuable information on its propulsion mechanisms (discussed later). Janus particles fabricated from polystyrene or silica microspheres (as opposed to PMMA) were also found to consistently move away from the AgCl side. Furthermore, PMMA–AgCl particles could also be activated by visible light (~0.1 W/cm^2) of wavelengths smaller than ~600 nm. A detailed description of particle dynamics at different lighting conditions is given in the Supporting Information (also Video S3).

To understand the dynamics of PMMA–AgCl micromotors, we first examine the chemical reaction occurring on their surfaces. When exposed to light of enough energy, AgCl decomposes into Ag, as follows[34,41]

$$4AgCl + 2H_2O = 4Ag + 4H^+ + 4Cl^- + O_2 \quad (1)$$

The conversion from AgCl into Ag on the particle surface is supported by crystalline and elemental composition characterization (Figure S2). Note that unlike a typical heterogeneous reaction where the concentration of a solid reactant is considered infinite, here, n_{AgCl} is finite and decreasing over time because the produced Ag coats back onto the particle and blocks further AgCl from reacting. The apparent reaction rate v [mol/(m^2 s)] of this photodecomposition averaged over the entire coated surface is therefore reasonably assumed to be linearly proportional to the amount of AgCl left on the bead (n_{AgCl}, in mol/m^2), and we obtain

$$v = -\frac{dn_{AgCl}}{dt} = kn_{AgCl} = \frac{d[H^+]}{dt} = \frac{d[Cl^-]}{dt} = J \quad (2)$$

where J is the ionic flux (same for H^+ and Cl^-, in mol/(m^2 s)), k is the reaction rate constant (s^{-1}), and t is time (s). This leads to first-order reaction kinetics

$$J = J_0\, e^{-kt} \quad (3)$$

Theories[39] and our own simulation (introduced later) both suggest that the particle speed U scales linearly with J. We then obtain

$$U = U_0\, e^{-kt} \quad (4)$$

where U_0 is the peak speed from which the motor decays over time. The particle speed profile over time in Figure 2d can be fit

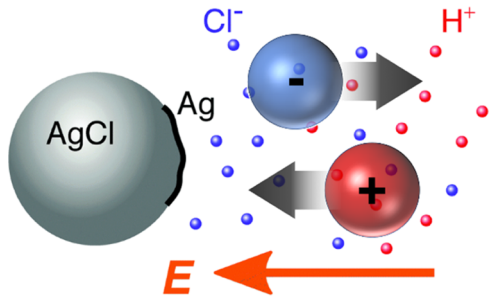

Figure 2. Typical picture of ionic diffusiophoresis near a photoactive AgCl microparticle. The produced H^+ diffuses faster than Cl^-, leading to an inward electric field that moves the nearby charged colloidal particles (large colored spheres). Adapted and modified from Figure 3 in ref 46 with permission from the Royal Society of Chemistry, 2017.

reasonably well by eq 4 (fit not shown), consistent with first-order kinetics. It is worth pointing out that the speeds of these Janus motors did not reach zero in the end, not because they were continuously but slowly propelled but rather because our tracking algorithm calculated an instantons speed of ~3 μm/s for Brownian motion. This, along with the observation that the speed decay profiles beyond ~5 s fit less well with exponential decays, is discussed in more detail in the Supporting Information.

The effect of solution conductivity (σ, tuned by adding different amounts of KNO_3 into the solution) is presented in Figure 1e (see Figure S3 for the full velocity data). Notably, micromotor peak speeds decreased significantly at high σ, qualitatively consistent with theories for an electrokinetic micromotor.[42−45] We also note that the photodecomposition of AgCl is a complicated multistep process involving hypochlorous acid (HClO) as an important intermediate, whose decomposition into O_2 is catalyzed by Ag^+.[41] However, adding a small amount (200 μM) of $AgNO_3$ in the solution did not significantly change the particle dynamics beyond the conductivity effect. Equation 1 is therefore considered appropriate for our discussion.

We now focus on the origin of the particle propulsion and particularly why it moved away from the AgCl-coated side. As mentioned earlier, the local and self-generated chemical gradients of the ionic species in eq 1 induce ionic self-diffusiophoresis (iSD). This mechanism is illustrated in Figure 2 (adapted from ref 46),[46] where a silver chloride (AgCl) microparticle decomposes into silver (Ag) when illuminated and releases protons (H^+) and chloride ions (Cl^-). Because H^+

DOI: 10.1021/acs.langmuir.7b04301
Langmuir 2018, 34, 3289−3295

diffuses much faster than Cl^- (diffusion coefficients 9.31×10^{-9} and 2.03×10^{-9} m^2/s, respectively), an inward electric field spontaneously forms to maintain charge neutrality in the bulk. Previously, this physical picture has been used to understand how nearby positively (negatively) charged microparticles were attracted toward (repelled from) the ion-releasing particle and how fascinating collective behaviors (such as schooling) emerged when every particle was active.[34]

However, how does the ion-releasing particle itself move? Figure 2 becomes less helpful in this regard because although it excels in explaining the pairwise interactions and collective behaviors among diffusiophoretic particles,[29,32,34,47−49] it looks at the electric field around the particle with a far-field approximation. If we, for example, consider the electric field depicted in Figure 2 that is pointing to the left, the electrophoretic motion of negatively charged PMMA−AgCl particles toward the AgCl side entails, whereas in our experiments they move in the opposite direction. As we have noted earlier, there is no satisfactory explanation/prediction in the literature on how the ion-releasing Janus particle moves because of various complications.

The solution to this inconsistency could lie in the distribution of electric and flow fields around the entirety of a moving Janus particle, including the near-field components, solved by finite element simulations (COMSOL Multiphysics, see Supporting Information for details). Specifically, the results in Figure 3a show a lower electrical potential near the AgCl cap

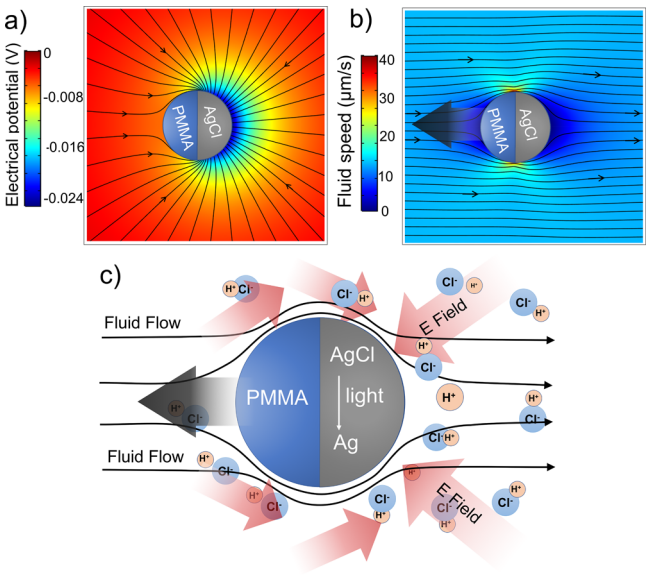

Figure 3. Finite element simulation of PMMA−AgCl micromotors. (a) Electrical potential (V, color-coded) and electric field (black arrows) distribution around a Janus particle. (b) Fluid speed magnitude (color-coded) and flow field lines (black arrows) in the reference frame of a Janus particle, which moves away from the AgCl side in the lab frame. (c) Schematics of how a PMMA−AgCl micromotor moves.

and an electric field that consequently points inward in the far field, both in agreement with Figure 2. However, the simulation also reveals additional electric field lines that point from the PMMA toward the AgCl hemisphere in the near field that, when coupled with the negative surface charges, create a slip velocity pointing in the same direction (Figure 3b). It is *this* slip flow, we argue, that causes the motor to move away from the AgCl side. Our refreshed operating mechanism of ionic self-diffusiophoresis is summarized in Figure 3c.

Not only is our model capable of explaining the directionality of Janus motors, it also solves for the motor speeds using the experimentally measured reaction rate constant k (see Supporting Information for details). Two major assumptions were made: (1) only a thin layer of AgCl participated in the reaction and (2) k (the reaction rate constant, acquired by fitting the speed profile for the first 3 s) remained unchanged during the reaction. An initial ion flux J of $\sim 1.6 \times 10^{-5}$ mol/(m^2 s) was then estimated, leading to particle speeds that decay exponentially from a peak speed of ~ 12 μm/s, which is roughly half of the experimental value shown in Figure 1d. Our simulation also suggests that the particle speed scales to J ($D_{H^+} - D_{Cl^-}$) (Figures S12 and S14), consistent with theories.[43] We acknowledge that the current numerical model is far from perfect and serves better as a qualitative guide than a quantitative prediction. Inaccuracies could stem from the much-simplified estimation of the amount of reactive AgCl or the fact that surface charges are prone to change as a result of surface reactions. Further improvements are under way.

To corroborate our proposed mechanism of ionic self-diffusiophoresis, we consider two complicating factors starting with possible mechanisms other than ionic self-diffusiophoresis that could contribute to the motion of PMMA−AgCl particles. For example, the produced O_2 (or HClO) in eq 1, one might argue, suggests the possibility of bubble propulsion or nonionic diffusiophoresis. Bubble propulsion, a mechanism responsible for a major category of micromotors that jet through water by bubble recoil,[50,51] can be readily eliminated because no bubble was observed in the vicinity of moving Janus particles. Nonionic diffusiophoresis, on the other hand, is a controversial issue,[43,44,52] and there is, to the best of our knowledge, no indisputable proof that the production of dissolved O_2 or HClO alone can propel micromotors at ~ 10 μm/s at the flux magnitude in our experiment. In addition, the observed scaling law between the particle speed and the solution conductivity in Figure 2e strongly suggests an electrokinetic effect. The contribution of nonionic products is therefore believed to be small.

One might also wonder if thermal effects contribute in the form of thermophoresis. This could be due to, for example, the photodecomposition of AgCl. However, numerical simulation shows a negligible temperature gradient across the particle from the reaction enthalpy change (endothermic, $\Delta H_f = 102.79$ kJ/mol) and reaction rates. Moreover, because AgCl is known to decompose in light, we do not expect it to show a strong photothermal effect. Ag nanoparticles, on the other hand, are known to show strong plasmonic resonance in the visible spectrum. However, thermophoresis due to photothermal Ag nanoparticles would lead to faster motors as the conversion from AgCl to Ag progressed, whereas the opposite speed profile was observed. We further confirm that neither PMMA−Ag Janus particles before conversion to AgCl nor PMMA−AgCl Janus particles after a long light exposure showed any directional motion beyond Brownian motion when irradiated with light (see Figure S7), strongly suggesting that the particle motion was associated with the decomposition of AgCl instead of thermal effects of Ag. The possible contributions from heat, bubbles, or nonionic diffusiophoresis, are therefore regarded as negligible as compared to the ionic diffusiophoresis mechanism we proposed.

DOI: 10.1021/acs.langmuir.7b04301
Langmuir 2018, 34, 3289−3295

Finally, we consider the bottom substrates that Janus particles reside on (or not, see below) and how it may or may not affect the particle dynamics. The boundary issue arises in light of recent studies that have shown how charged boundaries can significantly affect the speed and directionality of nearby phoretic micromotors via hydrodynamic, electrostatic, or phoretic effects.[38,39,53−55] One might then argue that this boundary effect also applies to PMMA−AgCl particles, which naturally sediment, and changes their speeds or directionality. The most straightforward response to this argument is to examine the particle dynamics in the bulk solution far away from any boundary, but this has been experimentally challenging because of the fact that Janus particles are often heavier than water and naturally sediment.

To address this issue, we designed an ultrasonically manipulated device to trap particles on a pressure nodal plane by megahertz acoustic standing waves (Figure 4a),[12,36]

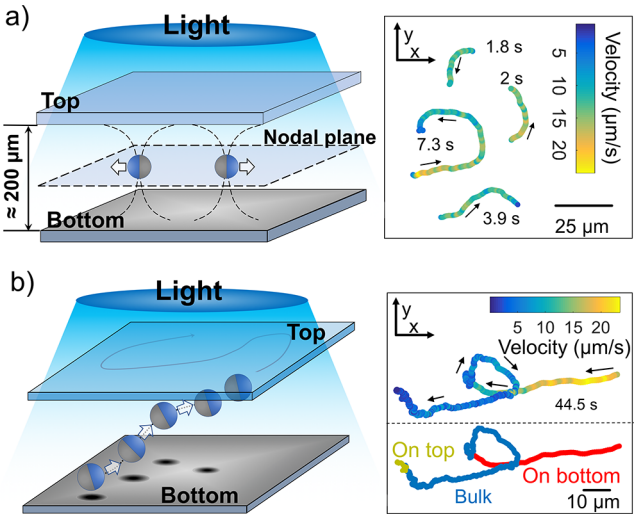

Figure 4. Effect of boundaries on light-driven PMMA−AgCl micromotors. (a) Motors are levitated by acoustic standing waves (dashed lines) and move in the bulk solution away from the AgCl side (silver color) after the ultrasound was turned off. A few representative trajectories are presented on the right, with particle velocities color-coded and time durations labeled. (b) Motors undergo gravitaxis under light and move from the bottom to the top of the experimental cell. One representative motor trajectory (44.5 s) from the bottom to the top of the cell is presented on the right.

the principle of which has been widely studied and exploited in the field of microfluidics and acoustofluidic devices.[56−58] On this levitation plane ∼100 μm away from either the top or bottom surface (Video S4), the illuminated PMMA−AgCl particles moved away from the AgCl side with speed profiles comparable to when they were near boundaries. These results strongly suggest that boundaries had a minor effect on either the speed or the directionality of AgCl Janus micromotors. Because the focus of the current study is on the individual dynamics of AgCl micromotors, we leave the discussion on this interesting and somewhat surprising insensitivity to walls to a future study.

An interesting consequence of the PMMA−AgCl micromotors moving away from the AgCl side is their negative gravitaxis (Figure 4b, Videos S5 and S6); some particles that were initially settled at the cell bottom could, when irradiated with strong light, rise up in the z direction and out of focus. In ∼10 s, they reached the top cell cover (cell height ≈ 200 μm), where they resumed 2D activity and gradually slowed down. A quantitative comparison between their dynamics at the bottom, in the bulk, and at the surface, however, is challenging because of the limitations of tracking techniques as well as their gradual loss in speeds. We also note that these gravitactic particles were not permanently trapped at the top boundary; they readily sediment if light was turned off or if their speeds decayed below a certain level (threshold not measured). Such a negative gravitaxis might be explained by a simple density argument: because AgCl has a higher density (5.56 g/cm^3) than water and PMMA (1.18 g/cm^3), the AgCl side of the Janus particle preferably orients toward the bottom and, when activated by light, propels the particle upward and away from the AgCl side. Such a preferred orientation was experimentally confirmed for PMMA−AgCl particles sedimented near a substrate under weak light, which shows a probability of 64.5% having the AgCl cap tilted downward (statistics acquired from 45 Janus spheres; see Supporting Information and Figure S8 for details).

Gravitactic micromotors were previously observed for chemically propelled Janus micromotors,[59,60] but light-induced negative gravitaxis opens up new and interesting possibilities. For example, one can imagine that these gravitactic micromotors act like scuba divers and can, when cued by light, transport cargos or analytes located at the bottom or in the bulk solution to the surface, where further analysis or assembly awaits. When the mission is finished or their service is no longer needed, particles dive back down, waiting to be summoned again. This kind of activated but independent "commute" between the bulk and an interface is significantly different from almost any kind of micromotors to date that only dwell near an interface, and could enable the autonomous yet controlled exploration of their three-dimensional (3D) environments. Although this vision is tempting, we acknowledge the limitation of the current AgCl micromotors such as their short lifetimes and long response times, both on the order of seconds. In addition, AgCl micromotors consume their active chemicals (AgCl) over time and are therefore not reusable or sustainable, although efforts on recycled micromotors based on silver halide have been reported.[61] Improvement of the photoactivated Janus micromotor and a more thorough study of its gravitactic effect are currently under way.

CONCLUSION

To summarize, we have developed a photoactive dielectric-AgCl Janus motor that, when illuminated with UV or strong visible light, moved away from the AgCl side and showed negative gravitaxis. The photodecomposition of AgCl into H^+ and Cl^- is believed to induce ionic self-diffusiophoresis, leading to an exponential speed decay. Through control experiments far from any boundaries, combined with finite element simulation, the moving direction of PMMA−AgCl micromotors is believed to be due to the near-field electrokinetic slip flow from the uncoated to the coated side. These motors also showed negative gravitaxis and creamed to the top surface when illuminated, a potentially useful feature for sensing applications and cargo transport in 3D. The current study improves our understanding of ionic self-diffusiophoresis and might shed light on the future designs of chemically powered micro- and nanomachines. Additionally, the unique benefit of acoustic levitation demonstrated in this study opens up great opportunities for studying active matter away from boundaries.

DOI: 10.1021/acs.langmuir.7b04301
Langmuir 2018, 34, 3289−3295

■ ASSOCIATED CONTENT

Supporting Information

The Supporting Information is available free of charge on the ACS Publications website at DOI: 10.1021/acs.langmuir.7b04301.

Multiple PMMA−AgCl Janus particles undergoing directional motion (AVI)

One PMMA−AgCl Janus particle undergoing directional motion under a mercury lamp (AVI)

Particle dynamics under six different lighting conditions (AVI)

Particle dynamics in the bulk (AVI)

Gravitaxis of Janus particles (AVI)

Particle dynamics at the cell "ceiling" (AVI)

Literature survey reports on ionic self-diffusiophoresis, figures of sample synthesis and particle dynamics at different experimental conditions, a brief discussion on the effect of different lighting conditions, numerical simulation details, and description of video files (PDF)

■ AUTHOR INFORMATION

Corresponding Author

*E-mail: weiwangsz@hit.edu.cn, wwang.hitsz@gmail.com.

ORCID

Jinyao Tang: 0000-0002-0051-148X

Wei Wang: 0000-0003-4163-3173

Funding

This project is financially supported by the National Natural Science Foundation of China (11774075, 11402069 and 11422427), the Natural Science Foundation of Guangdong Province (no. 2017B030306005), the Science Technology and Innovation Program of Shenzhen (JCYJ20170307150031119), and the Program for Professor of Special Appointment at Shanghai Institutions of Higher Learning Grant.

Notes

The authors declare no competing financial interest.

■ ACKNOWLEDGMENTS

The authors would like to thank Prof. Thomas Mallouk, Ayusman Sen, Darrell Velegol, John Gibbs, and Dr. Himanagamanasa Kandula for their extremely helpful discussions and Xiaobin Fan for the help with light power density measurement.

■ REFERENCES

(1) Ramaswamy, S. The Mechanics and Statistics of Active Matter. *Annu. Rev. Condens. Matter Phys.* **2010**, *1*, 323−345.

(2) Wang, J. *Nanomachines: Fundamentals and Applications*; John Wiley & Sons: Hoboken, 2013.

(3) Mallouk, T. E.; Sen, A. Powering Nanorobots. *Sci. Am.* **2009**, *300*, 72−77.

(4) Lauga, E.; Powers, T. R. The Hydrodynamics of Swimming Microorganisms. *Rep. Prog. Phys.* **2009**, *72*, 096601.

(5) Purcell, E. M. Life at Low Reynolds Number. *Am. J. Phys.* **1977**, *45*, 3−11.

(6) Peng, F.; Tu, Y.; Wilson, D. A. Micro/Nanomotors Towards in Vivo Application: Cell, Tissue and Biofluid. *Chem. Soc. Rev.* **2017**, *46*, 5289−5310.

(7) Li, J.; de Ávila, B. E.-F.; Gao, W.; Zhang, L.; Wang, J. Micro/Nanorobots for Biomedicine: Delivery, Surgery, Sensing, and Detoxification. *Sci. Robot.* **2017**, *2*, No. eaam6431.

(8) Jain, R. K.; Stylianopoulos, T. Delivering Nanomedicine to Solid Tumors. *Nat. Rev. Clin. Oncol.* **2010**, *7*, 653−664.

(9) Martel, S. Journey to the Center of a Tumor. *IEEE Spectrum* **2012**, *49*, 48−53.

(10) Fournier-Bidoz, S.; Arsenault, A. C.; Manners, I.; Ozin, G. A. Synthetic Self-Propelled Nanorotors. *Chem. Commun.* **2005**, 441−443.

(11) Paxton, W. F.; Kistler, K. C.; Olmeda, C. C.; Sen, A.; St. Angelo, S. K.; Cao, Y.; Mallouk, T. E.; Lammert, P. E.; Crespi, V. H. Catalytic Nanomotors: Autonomous Movement of Striped Nanorods. *J. Am. Chem. Soc.* **2004**, *126*, 13424−13431.

(12) Rao, K. J.; Li, F.; Meng, L.; Zheng, H.; Cai, F.; Wang, W. A Force to Be Reckoned With: A Review of Synthetic Microswimmers Powered by Ultrasound. *Small* **2015**, *11*, 2836−2846.

(13) Wang, W.; Duan, W.; Ahmed, S.; Mallouk, T. E.; Sen, A. Small Power: Autonomous Nano- and Micromotors Propelled by Self-Generated Gradients. *Nano Today* **2013**, *8*, 531−554.

(14) Xu, L.; Mou, F.; Gong, H.; Luo, M.; Guan, J. Light-Driven Micro/Nanomotors: From Fundamentals to Applications. *Chem. Soc. Rev.* **2017**, *46*, 6905−6926.

(15) Lin, X.; Si, T.; Wu, Z.; He, Q. Self-Thermophoretic Motion of Controlled Assembled Micro-/Nanomotors. *Phys. Chem. Chem. Phys.* **2017**, *19*, 23606−23613.

(16) Xu, T.; Gao, W.; Xu, L.-P.; Zhang, X.; Wang, S. Fuel-Free Synthetic Micro-/Nanomachines. *Adv. Mater.* **2016**, *29*, 1603250.

(17) Colberg, P. H.; Reigh, S. Y.; Robertson, B.; Kapral, R. Chemistry in Motion: Tiny Synthetic Motors. *Acc. Chem. Res.* **2014**, *47*, 3504−3511.

(18) Dey, K. K.; Sen, A. Chemically Propelled Molecules and Machines. *J. Am. Chem. Soc.* **2017**, *139*, 7666−7676.

(19) Sánchez, S.; Soler, L.; Katuri, J. Chemically Powered Micro- and Nanomotors. *Angew. Chem., Int. Ed.* **2015**, *54*, 1414−1444.

(20) Ebel, J. P.; Anderson, J. L.; Prieve, D. C. Diffusiophoresis of Latex Particles in Electrolyte Gradients. *Langmuir* **1988**, *4*, 396−406.

(21) Velegol, D.; Garg, A.; Guha, R.; Kar, A.; Kumar, M. Origins of Concentration Gradients for Diffusiophoresis. *Soft Matter* **2016**, *12*, 4686−4703.

(22) Popescu, M. N.; Uspal, W. E.; Dietrich, S. Self-Diffusiophoresis of Chemically Active Colloids. *Eur. Phys. J.: Spec. Top.* **2016**, *225*, 2189−2206.

(23) Guix, M.; Meyer, A. K.; Koch, B.; Schmidt, O. G. Carbonate-Based Janus Micromotors Moving in Ultra-Light Acidic Environment Generated by Hela Cells in Situ. *Sci. Rep.* **2016**, *6*, 21701.

(24) McDermott, J. J.; Kar, A.; Daher, M.; Klara, S.; Wang, G.; Sen, A.; Velegol, D. Self-Generated Diffusioosmotic Flows from Calcium Carbonate Micropumps. *Langmuir* **2012**, *28*, 15491−15497.

(25) Gáspár, S. Enzymatically Induced Motion at Nano- and Micro-Scales. *Nanoscale* **2014**, *6*, 7757−7763.

(26) Ma, X.; Hortelão, A. C.; Patiño, T.; Sánchez, S. Enzyme Catalysis to Power Micro/Nanomachines. *ACS Nano* **2016**, *10*, 9111−9122.

(27) Dey, K. K.; Zhao, X.; Tansi, B. M.; Méndez-Ortiz, W. J.; Córdova-Figueroa, U. M.; Golestanian, R.; Sen, A. Micromotors Powered by Enzyme Catalysis. *Nano Lett.* **2015**, *15*, 8311−8315.

(28) Ma, X.; Jannasch, A.; Albrecht, U.-R.; Hahn, K.; Miguel-López, A.; Schäffer, E.; Sánchez, S. Enzyme-Powered Hollow Mesoporous Janus Nanomotors. *Nano Lett.* **2015**, *15*, 7043−7050.

(29) Hong, Y.; Diaz, M.; Córdova-Figueroa, U. M.; Sen, A. Light-Driven Titanium-Dioxide-Based Reversible Microfireworks and Micromotor/Micropump Systems. *Adv. Funct. Mater.* **2010**, *20*, 1568−1576.

(30) Chen, C.; Mou, F.; Xu, L.; Wang, S.; Guan, J.; Feng, Z.; Wang, Q.; Kong, L.; Li, W.; Wang, J.; Zhang, Q. Semiconductors: Light-Steered Isotropic Semiconductor Micromotors. *Adv. Mater.* **2017**, *29*, 163374.

(31) Chen, H.; Zhao, Q.; Du, X. Light-Powered Micro/Nanomotors. *Micromachines* **2018**, *9*, 41.

(32) Sen, A.; Ibele, M.; Hong, Y.; Velegol, D. Chemo and Phototactic Nano/Microbots. *Faraday Discuss.* **2009**, *143*, 15−27.

DOI: 10.1021/acs.langmuir.7b04301
Langmuir 2018, 34, 3289−3295

(33) Chaturvedi, N.; Hong, Y.; Sen, A.; Velegol, D. Magnetic Enhancement of Phototaxing Catalytic Motors. *Langmuir* **2010**, *26*, 6308−6313.
(34) Ibele, M.; Mallouk, T. E.; Sen, A. Schooling Behavior of Light-Powered Autonomous Micromotors in Water. *Angew. Chem., Int. Ed.* **2009**, *48*, 3308−3312.
(35) Goldenberg, L. M.; Wagner, J.; Stumpe, J.; Paulke, B.-R.; Görnitz, E. Simple Method for the Preparation of Colloidal Particle Monolayers at the Water/Alkane Interface. *Langmuir* **2002**, *18*, 5627−5629.
(36) Wang, W.; Castro, L. A.; Hoyos, M.; Mallouk, T. E. Autonomous Motion of Metallic Microrods Propelled by Ultrasound. *ACS Nano* **2012**, *6*, 6122−6132.
(37) Kline, T. R.; Iwata, J.; Lammert, P. E.; Mallouk, T. E.; Sen, A.; Velegol, D. Catalytically Driven Colloidal Patterning and Transport. *J. Phys. Chem. B* **2006**, *110*, 24513−24521.
(38) Chiang, T.-Y.; Velegol, D. Localized Electroosmosis (LEO) Induced by Spherical Colloidal Motors. *Langmuir* **2014**, *30*, 2600−2607.
(39) Liu, C.; Zhou, C.; Wang, W.; Zhang, H. P. Bimetallic Microswimmers Speed up in Confining Channels. *Phys. Rev. Lett.* **2016**, *117*, 198001.
(40) Bi, Y.; Ye, J. In Situ Oxidation Synthesis of Ag/AgCl Core-Shell Nanowires and Their Photocatalytic Properties. *Chem. Commun.* **2009**, 6551−6553.
(41) Calzaferri, G. At the Time He Made the First Photographs on Paper: Did Henry Fox Talbot Oxidize Water to Oxygen with Sunlight? *Catal. Today* **1997**, *39*, 145−157.
(42) Paxton, W. F.; Baker, P. T.; Kline, T. R.; Wang, Y.; Mallouk, T. E.; Sen, A. Catalytically Induced Electrokinetics for Motors and Micropumps. *J. Am. Chem. Soc.* **2006**, *128*, 14881−14888.
(43) Brown, A. T.; Poon, W. C. K.; Holm, C.; de Graaf, J. Ionic Screening and Dissociation Are Crucial for Understanding Chemical Self-Propulsion in Polar Solvents. *Soft Matter* **2017**, *13*, 1200−1222.
(44) Brown, A.; Poon, W. Ionic Effects in Self-Propelled Pt-Coated Janus Swimmers. *Soft Matter* **2014**, *10*, 4016−4027.
(45) Moran, J. L.; Posner, J. D. Role of Solution Conductivity in Reaction Induced Charge Auto-Electrophoresis. *Phys. Fluids* **2014**, *26*, 042001.
(46) Illien, P.; Golestanian, R.; Sen, A. "Fuelled" motion: Phoretic Motility and Collective Behaviour of Active Colloids. *Chem. Soc. Rev.* **2017**, *46*, 5508−5518.
(47) Ibele, M. E.; Lammert, P. E.; Crespi, V. H.; Sen, A. Emergent, Collective Oscillations of Self-Mobile Particles and Patterned Surfaces under Redox Conditions. *ACS Nano* **2010**, *4*, 4845−4851.
(48) Duan, W.; Liu, R.; Sen, A. Transition between Collective Behaviors of Micromotors in Response to Different Stimuli. *J. Am. Chem. Soc.* **2013**, *135*, 1280−1283.
(49) Altemose, A.; Sánchez-Farrán, M. A.; Duan, W.; Schulz, S.; Borhan, A.; Crespi, V. H.; Sen, A. Chemically-Controlled Spatiotemporal Oscillations of Colloidal Assemblies. *Angew. Chem.* **2017**, *129*, 7925−7929.
(50) Mei, Y.; Huang, G.; Solovev, A. A.; Ureña, E. B.; Mönch, I.; Ding, F.; Reindl, T.; Fu, R. K. Y.; Chu, P. K.; Schmidt, O. G. Versatile Approach for Integrative and Functionalized Tubes by Strain Engineering of Nanomembranes on Polymers. *Adv. Mater.* **2008**, *20*, 4085−4090.
(51) Magdanz, V.; Guix, M.; Schmidt, O. G. Tubular Micromotors: From Microjets to Spermbots. *Rob. Biomimetics* **2014**, *1*, 11.
(52) Ebbens, S.; Gregory, D. A.; Dunderdale, G.; Howse, J. R.; Ibrahim, Y.; Liverpool, T. B.; Golestanian, R. Electrokinetic Effects in Catalytic Platinum-Insulator Janus Swimmers. *Europhys. Lett.* **2014**, *106*, 58003.
(53) Uspal, W. E.; Popescu, M. N.; Dietrich, S.; Tasinkevych, M. Self-Propulsion of a Catalytically Active Particle near a Planar Wall: From Reflection to Sliding and Hovering. *Soft Matter* **2015**, *11*, 434−438.
(54) Das, S.; Garg, A.; Campbell, A. I.; Howse, J.; Sen, A.; Velegol, D.; Golestanian, R.; Ebbens, S. J. Boundaries Can Steer Active Janus Spheres. *Nat. Commun.* **2015**, *6*, 8999.
(55) Simmchen, J.; Katuri, J.; Uspal, W. E.; Popescu, M. N.; Tasinkevych, M.; Sánchez, S. Topographical Pathways Guide Chemical Microswimmers. *Nat. Commun.* **2016**, *7*, 10598.
(56) Gröschl, M. Ultrasonic Separation of Suspended Particles-Part I: Fundamentals. *Acta Acust. Acust.* **1998**, *84*, 432−447.
(57) Evander, M.; Nilsson, J. Acoustofluidics 20: Applications in Acoustic Trapping. *Lab Chip* **2012**, *12*, 4667−4676.
(58) Shi, J.; Ahmed, D.; Mao, X.; Lin, S.-C. S.; Lawit, A.; Huang, T. J. Acoustic Tweezers: Patterning Cells and Microparticles Using Standing Surface Acoustic Waves (SSAW). *Lab Chip* **2009**, *9*, 2890−2895.
(59) Takatori, S. C.; De Dier, R.; Vermant, J.; Brady, J. F. Acoustic Trapping of Active Matter. *Nat. Commun.* **2016**, *7*, 10694.
(60) Campbell, A. I.; Ebbens, S. J. Gravitaxis in Spherical Janus Swimming Devices. *Langmuir* **2013**, *29*, 14066−14073.
(61) Wong, F.; Sen, A. Progress toward Light-Harvesting Self-Electrophoretic Motors: Highly Efficient Bimetallic Nanomotors and Micropumps in Halogen Media. *ACS Nano* **2016**, *10*, 7172−7179.

DOI: 10.1021/acs.langmuir.7b04301
Langmuir 2018, 34, 3289−3295